analytical chemistry

Article

pubs.acs.org/ac

Analyzing Protein Micro-Heterogeneity in Chicken Ovalbumin by High-Resolution Native Mass Spectrometry Exposes Qualitatively and Semi-Quantitatively 59 Proteoforms

Yang Yang,[†,‡] Arjan Barendregt,[†,‡] Johannis P. Kamerling,[†] and Albert J. R. Heck*[,†,‡]

[†]Biomolecular Mass Spectrometry and Proteomics, Bijvoet Center for Biomolecular Research and Utrecht Institute for Pharmaceutical Sciences, University of Utrecht, Padualaan 8, 3584 CH Utrecht, The Netherlands

[‡]Netherlands Proteomics Center, Padualaan 8, 3584 CH Utrecht, The Netherlands

Supporting Information

ABSTRACT: Taking chicken Ovalbumin as a prototypical example of a eukaryotic protein we use high-resolution native electrospray ionization mass spectrometry on a modified Exactive Orbitrap mass analyzer to qualitatively and semi-quantitatively dissect 59 proteoforms in the natural protein. This variety is largely induced by the presence of multiple phosphorylation sites and a glycosylation site that we find to be occupied by at least 45 different glycan structures. Mass analysis of the intact protein in its native state is straightforward and fast, requires very little sample preparation, and provides a direct view on the stoichiometry of all different coappearing modifications that are distinguishable in mass. As such, this proof-of-principal analysis shows that native electrospray ionization mass spectrometry in combination with an Orbitrap mass analyzer offers a means to characterize proteins in a manner highly complementary to standard bottom-up shot-gun proteome analysis.

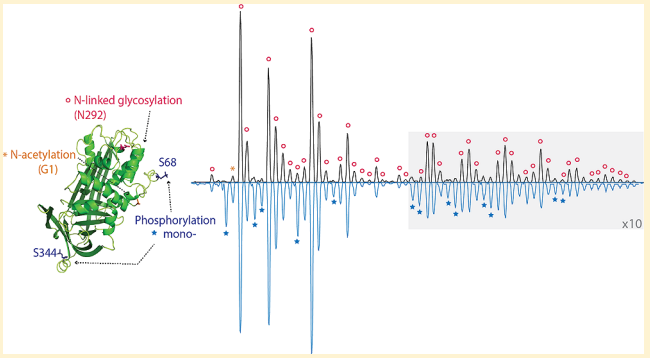

Ovalbumin is the most prominent protein found in egg white, making up 60−65% of the total protein mass. Although the exact function of ovalbumin is unknown, it is generally assumed to be a storage protein. Chicken ovalbumin consists of 385 amino acids and has a molecular mass of around 45 kDa. Ovalbumin is decorated by a plethora of post-translational modifications (PTMs), including N-terminal acetylation (G1), phosphorylation (most prominent at S68 and S344), and extensive glycosylation (N292) and contains a disulfide bridge (C73-Cys120).[1,2] Due to its availability, ovalbumin has often been used as a model system for new developments in the separation sciences, such as liquid chromatography,[3,4] capillary electrophoresis,[5,6] and mass spectrometry.[7] Ovalbumin does however represent quite an analytical challenge, due to the high and diverse amount of PTMs. In most of the reported analyses on the intact protein to date, the molecular heterogeneity of ovalbumin hampers a complete analysis of all different isoforms/proteoforms.[8] Therefore, so far the most successful strategies employed cleave the ovalbumin protein first into segments, followed by analysis of the resulting peptides and glycopeptides, or to release the glycans from generated glycopeptides or denatured protein. In this way, from the glycan analysis, a reasonable comprehensive view of the molecular complexity of the glycan structures present on ovalbumin has become available. Bottom-up peptide analysis by mass spectrometry provides a good qualitative and semiquantitative view of the phosphorylation sites occupied in ovalbumin. Yet, all these approaches require a variety of sample preparation steps, which may all inherently lead to loss of particular signals.

Recently, we introduced a modified version of an Orbitrap mass analyzer, adapted to be able to analyze large biomolecules and molecular assemblies.[9] A nice feature of this instrument is that it allows high mass accuracy and high resolving power of ions also in the m/z range way above m/z 2000, enabling analysis of biomolecules and biomolecular assemblies by electrospray ionization under native conditions. We previously showed that this instrument allows the analysis of intact proteasome and GroEL assemblies (M_w 700−800 kDa), and enables the mass distinction between different stoichiometries of nucleotide (i.e., ATP, ADP) binding to GroEL.[9] To further benchmark the possibilities of this instrument for the robust and efficient analysis of proteins, we focus now on the mass analysis of the chicken ovalbumin protein. The here presented native electrospray ionization (ESI) mass spectra of intact ovalbumin highlight this microheterogeneity, as mentioned above, in its full qualitative and quantitative glory, whereby we are able to detect, identify, and semiquantify at least 59 different proteoforms. This approach provides to the best of our

Received: September 24, 2013
Accepted: November 14, 2013
Published: November 14, 2013

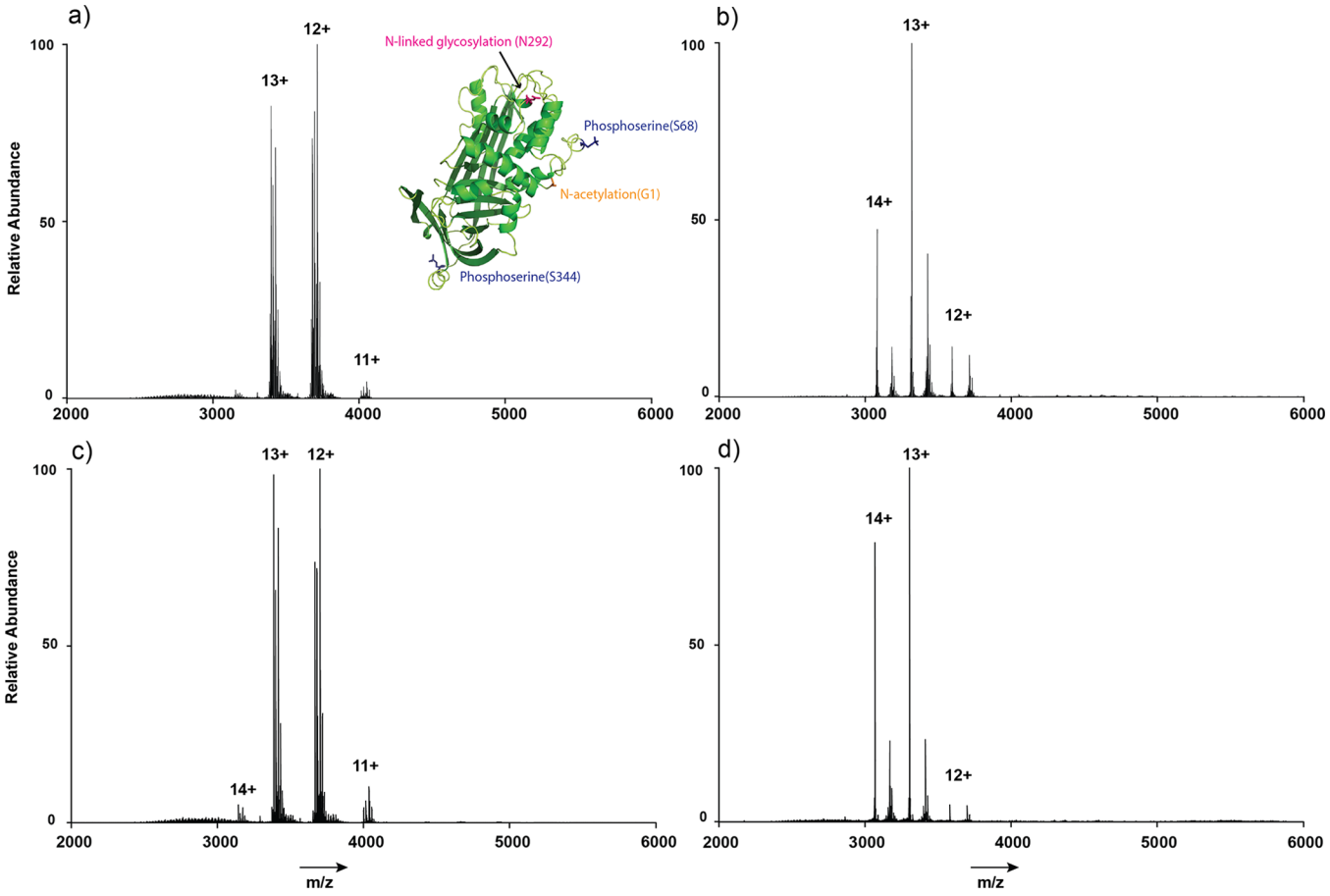

Figure 1. Full native ESI-MS spectra acquired on a modified Orbitrap Exactive of (a) unprocessed, (b) deglycosylated, (c) dephosphorylated and (d) deglycosylated and dephosphorylated ovalbumin from m/z 2000 to 6000. There are two series of proteoforms present in the spectra displayed in (b) and (d) because the deglycosylation is incomplete due to enzyme specificity of Endo F1. The inset shows the crystal structure of chicken ovalbumin with the two reported phosphorylation sites, the N-acetylated terminus and the glycosylation site annotated.

knowledge the most comprehensive analysis of proteoforms of ovalbumin to date. Moreover, the approach presented here is generic and can be adapted to analyze protein microheterogeneity in structural proteins, kinases, phosphatases, etc.

MATERIALS AND METHODS

Materials. Chicken ovalbumin (grade V) and Endoglycosidase F1 (Endo F1) were acquired from Sigma-Aldrich (Steinheim, Germany). Ovalbumin consists of 385 amino acids (Uniprot Code P01012, sequence mass 42750.19 kDa). Calf Intestinal Alkaline Phosphatase (CIP) was obtained from New England BioLabs (Beverly, MA).

Sample Preparation. Unprocessed ovalbumin solutions were prepared at a concentration of 200 μM in milli-Q water and then buffer exchanged into 150 mM aqueous ammonium acetate (AmAc) (pH 7.5). Enzymatic dephosphorylation was performed by incubating unprocessed ovalbumin with CIP in 50 mM triethyl ammonium bicarbonate (TEAB) buffer (pH 7.5) at 37 °C for 2 h. The protein/enzyme ratio was 0.5 units of CIP per 1 μg protein. Enzymatic deglycosylation was performed by incubating 0.2 units Endo F1 with 200 μg ovalbumin in a reaction buffer (20 mM Tris-HCl, pH 7.5, provided with the enzyme kit) at 37 °C overnight. Deglycosylated ovalbumin was buffer exchanged into aqueous AmAc buffer prior to CIP dephosphorylation.

Prior to mass spectrometry (MS) analysis, the protein samples were exchanged into 150 mM aqueous AmAc (pH 7.5) by ultrafiltration (vivaspin500, Sartorius Stedim Biotech, Germany) with a 5 kDa cutoff. The protein concentration was measured by UV absorbance at 280 nm and adjusted to 2−3 μM before MS measurement.

Native MS Analysis on the Orbitrap Mass Analyzer. One to two microliters of individual sample was loaded into a nanoflow gold-plated borosilicate electrospray capillary (made in house). The sample was analyzed on a modified Exactive Plus instrument (Thermo Fisher Scientific, Bremen, Germany) over m/z range 500−10000, as described previously.[9] On the basis of the length of the transients observed, the Orbitrap resolution was set to 17500 at m/z 200. Nitrogen was used in the HCD cell and gas pressure was manually regulated. The voltage offset on transport multiples and ion lenses were manually tuned to achieve optimal transmission of protein ions at elevated m/z. The instrument was calibrated by using CsI clusters, as described previously.[9]

Data Processing. The accurate masses of the observed proteoforms were obtained by convoluting the ESI spectrum to a zero-charge state spectrum using the Protein Deconvolution package (Thermo Fisher Scientific). For glycan assignment, the reference molecular weights of 5 monosaccharides were extracted from the GlycosuiteDB (ExPAsy), and a tolerance rate (0.015) was set to give an acceptable mass range of reference. After building a mass difference matrix between any

dx.doi.org/10.1021/ac403057y | Anal. Chem. 2013, 85, 12037−12045

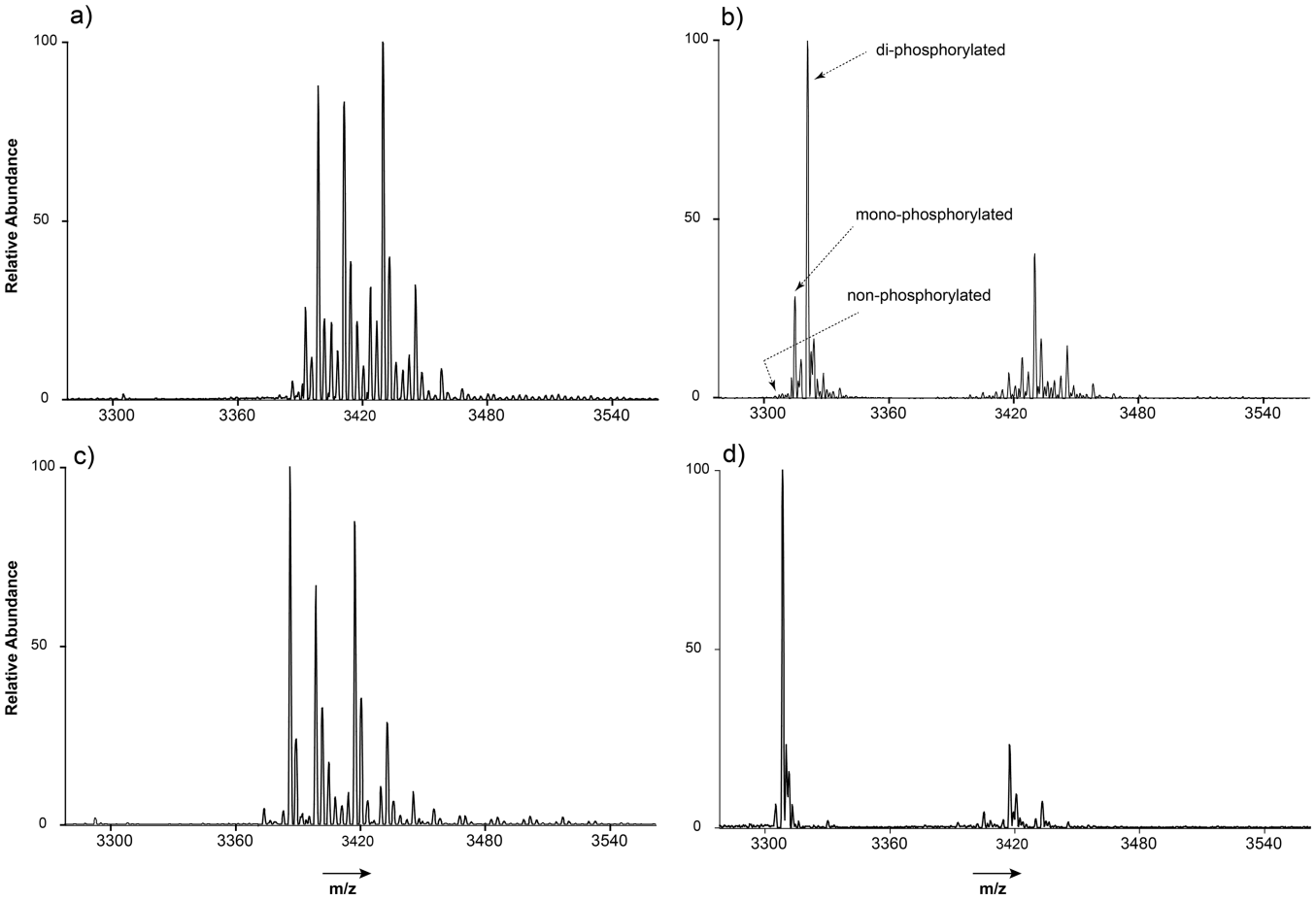

Figure 2. Zoom in on the $[M + 13H]^{13+}$ charge state, native ESI-MS spectra of (a) unprocessed, (b) deglycosylated, (c) dephosphorylated, and (d) deglycosylated and dephosphorylated ovalbumin. From a comparison of the spectra in (b) and (d), the two phosphorylation sites could be confirmed. The average mass of the "naked" ovalbumin polypeptide backbone (with N-acetylation, and one GlcNAc) determined from the spectrum (d) is 42995.35 Da, within 1.23 ppm of the expected mass (42995.29 Da). The abundance ratio between the maximum and minimum detectable and assigned proteoforms is ~800.

two of the detected masses on the dephosphorylated ovalbumin spectrum, we consider any element that falls in one of the set masses as a match. Glycan structures were built based on known biosynthetic pathways and reported ovalbumin literature and were drawn using GlycoBench.[10] The reference monosaccharides used were hexose/mannose/galactose (Hex/Man/Gal, 162.1424 Da), *N*-acetylhexosamine/*N*-acetylglucosamine (HexNAc/GlcNAc, 203.1950 Da), deoxyhexose (dHex, 146.1430 Da), *N*-acetylneuraminic acid (Neu5Ac, 291.2579 Da), and *N*-glycolylneuraminic acid (Neu5Gc, 307.2573 Da), according to symbol and text nomenclature from the Consortium for Functional Glycomics.

RESULTS

Preparation of Dephosphorylated and/or Deglycosylated Ovalbumin. Enzymatic removal of PTMs potentially simplifies the variety of proteoforms and thus the resulting MS spectra, providing necessary information for elucidating coappearing proteoforms. For dephosphorylation, it is possible to remove all the phosphate groups from ovalbumin using CIP. In the case of deglycosylation, the generally used *N*-glycosidase F (PNGase F) for the cleavage of GlcNAc-Asn linkages in denatured N-glycoproteins, thereby releasing the attached ensemble of N-glycans, turned out to be ineffective for ovalbumin under native conditions (data not shown). Probably the GlcNAc-Asn linkage is not easily accessible in the ovalbumin native conformation. Inspection of the crystal structure of uncleaved ovalbumin showed that the glycosylation site N292 is located in the loop between an α helix and a β strand.[11] The GlcNAc-Asn292 linkage could be tightly packed in the native ovalbumin conformation, making it difficult for PNGase F to approach.

As we would like to avoid denaturing conditions,[12] we explored the use of endo-β-*N*-acetylglucosaminidases, and we found that endo F1 was less sensitive to the ovalbumin conformation and therefore more suitable for deglycosylation. Endo F1 releases oligomannose- and hybrid-type N-glycans, provided that no intersecting GlcNAc is present, generating an ovalbumin form with one GlcNAc residue remaining on the Asn residue.[13−15] In accordance with our experiments, not all glycans were removed from the intact ovalbumin by Endo F1, but we could use this enzyme specificity to assist our glycan assignments.

Analysis of Dephosphorylated and Deglycosylated Ovalbumin. We measured the (a) natural unprocessed, (b) deglycosylated, (c) dephosphorylated, (d) deglycosylated and dephosphorylated ovalbumin by native mass spectrometry using the modified Orbitrap Exactive. The resulting four spectra are depicted in Figure 1 (panels a−d). Signals were averaged only for a few minutes, consuming a few femtomole of sample.

dx.doi.org/10.1021/ac403057y | *Anal. Chem.* 2013, 85, 12037−12045

Table 1. Quantitative Glycan Profiling of Chicken Ovalbumin[a]

no.	mass (Da)	relative abundance %	composition[b]	glycan (Da)	ref (Da)	deviation (Da)	structure[c]	ref[d]
1	43848.35	3.99	$Hex_4HexNAc_2$	1074.32	1072.95	1.38	+	26,29,39,47
2	44010.59	91.83	$Hex_5HexNAc_2$	1236.56	1235.09	1.47	+	24,31,37,39,42,47
3	44047.12	24.76	$Hex_4HexNAc_3$	1273.09	1276.14	3.05	+	47
4	44171.01	74.12	$Hex_6HexNAc_2$	1396.98	1397.23	0.25	+	24,31,35,37,42,47
5	44211.57	35.37	$Hex_5HexNAc_3$	1437.54	1438.28	0.74	+	47,52
6	44252.13	18.89	$Hex_4HexNAc_4$	1478.10	1479.34	1.23	+	35,37,42,47,52
7	44292.56	8.13	$Hex_3HexNAc_5$	1518.53	1520.40	1.87	+	32,35,37,42,47
8	44333.64	6.02	$Hex_7HexNAc_2$	1559.61	1559.37	0.24	+	25,34,37,39,42,47
9	44374.07	8.51	$Hex_6HexNAc_3$	1600.04	1600.42	0.38	+	47
10	44415.46	100.00	$Hex_5HexNAc_4$	1641.43	1641.48	0.05	+	25,31,37,39,47,52
11	44454.94	46.13	$Hex_4HexNAc_5$	1680.91	1682.53	1.62	+	25,34,37,39,42,47
12	44494.04	8.81	$Hex_3HexNAc_6$	1720.01	1723.60	3.59	+	32,39,47
13	44577.60	9.87	$Hex_6HexNAc_4$	1803.58	1803.62	0.04		–
14	44618.60	33.22	$Hex_5HexNAc_5$	1844.57	1844.67	0.10	+	27,37,39,47
15	44656.56	8.32	$Hex_4HexNAc_6$	1882.53	1885.73	3.19	+	34,39,47
16	44698.16	2.89	$Hex_3HexNAc_7$	1924.13	1926.79	2.66	+	47
17	44740.27	1.34	$Hex_7HexNAc_4$	1966.24	1965.76	0.48		–
18	44780.97	9.61	$Hex_6HexNAc_5$	2006.94	2006.81	0.13	+	27,31,37,39,47
19	44816.14	1.81	$HeX_5HexNAc_6$	2042.11	2047.88	5.77	+	47
20	44909.27	4.38	$Sia_1Hex_3HexNAc_5$	2135.24	2135.77	0.53		–
21	44947.26	2.04	$Sia_1Hex_4HexNAc_6$	2173.23	2176.82	3.59		–
22	44981.91	0.47	$Hex_6HexNAc_6$	2207.88	2210.01	2.13	+	47
23	45071.09	2.62	$Sia_1Hex_6HexNAc_5$	2297.06	2297.91	0.85	+	36
24	45105.92	2.52	$Sia_1Hex_5HexNAc_6$	2331.89	2338.96	7.07		–
25	45143.66	0.74	$Hex_7HexNAc_6$	2369.63	2372.15	2.52	+, G	20*
26	45199.09	0.20	$Sia_2Hex_5HexNAc_5$	2425.06	2426.86	1.80		–
27	45267.54	1.89	$Sia_1Hex_6HexNAc_6$	2493.51	2501.11	7.59	+, G	20*
28	45307.79	2.04	$Hex_8HexNAc_6$	2533.76	2534.29	0.53	+	20*
29	45348.27	0.94	$Hex_7HexNAc_7$	2574.24	2575.35	1.11		–
30	45470.87	1.28	$Hex_9HexNAc_6$	2696.85	2696.44	0.41	+, G	20*
31	45511.56	2.42	$Hex_8HexNAc_7$	2737.53	2737.49	0.04		–
32	45551.56	1.52	$Hex_7HexNAc_8$	2777.53	2778.54	1.01		–
33	45632.73	0.32	$Hex_{10}HexNAc_6$	2858.70	2858.58	0.12	+, G	–
34	45673.76	0.64	$Hex_9HexNAc_7$	2899.74	2899.63	0.10	+, G	20*
35	45714.78	2.27	$Hex_8HexNAc_8$	2940.75	2940.68	0.06		–
36	45753.97	1.00	$Hex_7HexNAc_9$	2979.94	2981.74	1.80		–
37	45835.80	0.28	$Hex_{10}HexNAc_7$	3061.78	3061.77	0.00	+, G	20*
38	45877.05	0.80	$Hex_9HexhNAc_8$	3103.03	3102.83	0.20		–
39	45917.96	1.00	$Hex_8HexNAc_9$	3143.93	3143.88	0.05		–
40	46001.66	0.23	$Sia_1Hex_8HexNAc_8$	3227.64	3231.78	4.14		–
41	46039.44	0.27	$Hex_{10}HexNAc_8$	3265.41	3264.97	0.44		–
42	46080.34	0.50	$Hex_9HexNAc_9$	3306.31	3306.02	0.29		–
43	46120.66	0.62	$Hex_8HexNAc_{10}$	3346.64	3347.07	0.44		–
44	46203.77	0.16	$Sia_1Hex_8HexNAc_9$	3429.74	3434.98	5.23	+, G	20*
45	46241.18	0.13	$Hex_{10}HexNAc_9$	3467.16	3468.16	1.01		–

[a]Mass and relative abundance of each detected and annotated proteoform are listed. The table also includes the proposed glycan compositions in terms of Hex (hexose; galactose/Gal + mannose/Man), HexNAc (*N*-acetylhexosamine; *N*-acetylglucosamine/GlcNAc), and Sia (sialic acid; *N*-acetylneuraminic acid/Neu5Ac), calculated glycan mass, its deviation from the expected mass, and its relative abundance, all extracted from a single native ESI-MS spectrum. Additionally, a list of references, corresponding to earlier established ovalbumin glycan structures (see Figure S-3 of the Supporting Information), is presented. [b]For the interpretation from composition to glycan structures, see Figures S-2, 3, and 4 of the Supporting Information. [c]In this column, "+" refers to all cases wherein at least one structure was reported. Meanwhile, the possible "unusual" moieties in chicken ovalbumin glycan structures are highlighted: "G" refers to the Gal(αl-4)Gal unit. [d]Asterisked ref is for pigeon ovalbumin, the rest are for chicken ovalbumin. Compositions with no previous annotation are marked with "–".

Whereas ESI under denaturing conditions results in ovalbumin ions with charge states between $[M + 18H]^{18+}$ and $[M + 45H]^{45+}$ (Figure S-1b of the Supporting Information), ESI under native conditions results in ovalbumin ions with signals primarily concentrated (over 95%) in only two charge states, increasing the signal-to-noise ratio (S/N), reducing potential overlap between different species, and facilitating convolution to a zero-charge mass spectrum. The high S/N ratio (~11000) in these spectra allows us to detect low abundant proteoforms next to the highest abundant ones. Practically, the ratio in abundance between the highest and lowest abundant assigned proteoforms was 800 (i.e., 0.1% relative to the base peak), a reasonable dynamic range in terms of native MS.

dx.doi.org/10.1021/ac403057y | *Anal. Chem.* 2013, 85, 12037−12045

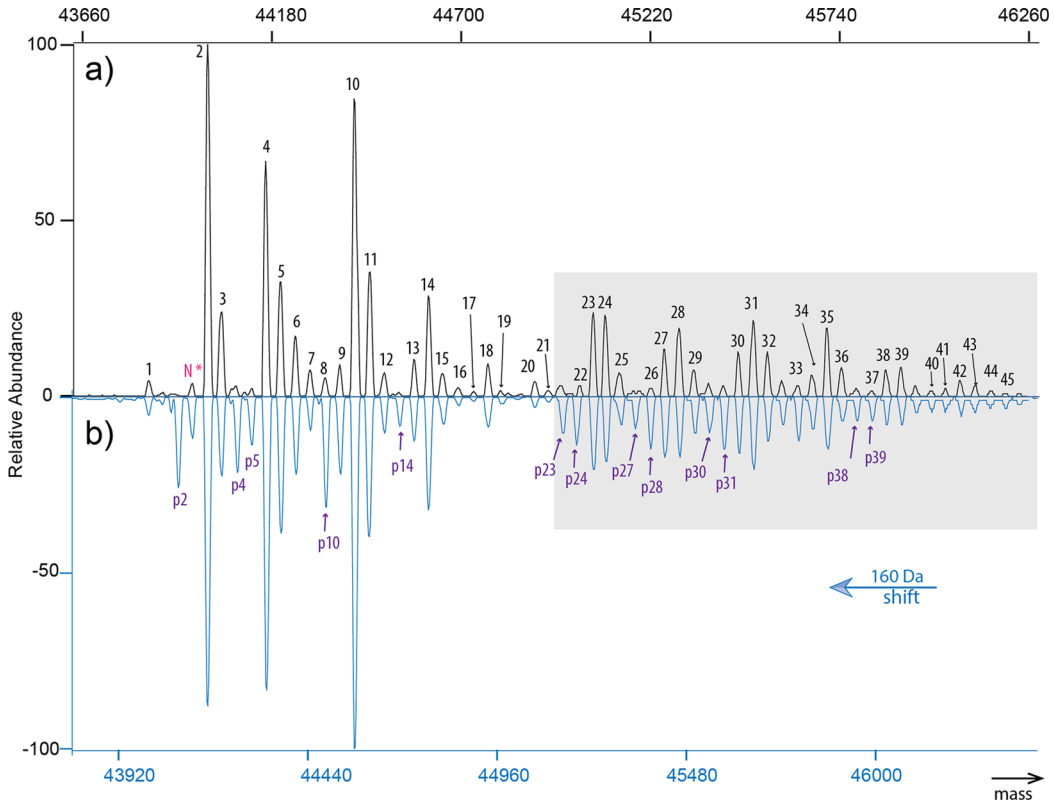

Figure 3. Characterization of 59 proteoforms in chicken ovalbumin. (a) Variations caused by the widespread glycosylation could be most easily identified and assigned using the spectrum of dephosphorylated ovalbumin. By comparing this spectrum in (a) to unprocessed ovalbumin in (b), proteoforms with either one or two phosphorylation sites occupied could be detected (with the single phosphorylated peaks annotated in purple). The proteoform lacking N-terminal acetylation is marked as N* in pink. The signals in the gray box are multiplied by a factor of 10 and highly enriched in the less reported glycan structures. We hypothesize that several of the complex-type glycans in the composition range 24−45 are in fact extensions of the well-established complex-type glycans from the composition range 1−23, namely, with terminal Gal(α1−4)Gal and polylactosamine units, in separated or mixed form.

In Figure 2, we zoom in looking only at the signals of the $[M + 13H]^{13+}$ ions, with again (a) the natural unprocessed, (b) deglycosylated, (c) dephosphorylated, (d) deglycosylated and dephosphorylated ovalbumin. Focusing first on the least composite spectrum of the deglycosylated and dephosphorylated ovalbumin in Figure 2d, we can extract from the most intense signal (at m/z 3300) the ovalbumin protein polypeptide backbone mass, without the decoration of glycosylation and phosphorylation. The mass of the polypeptide backbone of ovalbumin can be derived from the DNA[16] sequence to be 42750.19 Da. In our analysis after the removal of glycans by Endo F1 and the phosphates by CIP, there are still an N-acetylation (42.01 Da) and a GlcNAc residue (203.1950 Da) attached to the polypeptide chain. The experimentally measured mass is 42995.35 Da, which deviates by only 1.23 ppm from the predicted mass, taking these latter modifications into account (42995.28 Da). In Figure 2d, only a few other signals are observed, all of which can be assigned. In agreement with previous studies, ovalbumin is predominantly acetylated at the protein N-terminal;[17] however, our data also indicate the presence of a proteoform (42953.30 Da) lacking the N-acetylation (delta mass 42.05 Da), with a relative abundance of 6.20% compared to the N-acetylated species. In accordance with literature,[13] we found that not all glycans could be removed by Endo F1, resulting in several residual ion signals around m/z 3420. The result is in agreement with the statement of Endo F1 specificity, wherein high-mannose type (numbered 1, 2, 4, and 8) and hybrid type (numbered 3, 5, and 9) glycans have been completely released (cleavage GlcNAc−GlcNAc linkage), leaving hybrid-type glycans with intersecting GlcNAc and complex-type di-, tri-, and tetra-antennary structures (numbered 6, 7, 10−16, and 18−45).

Analysis of Deglycosylated Ovalbumin. After deglycosylation by Endo F1, the spectrum being presented in Figure 2b was recorded, wherein the number of coappearing proteoforms is clearly reduced (compare Figure 2, panels b and a), facilitating to extract data regarding the protein phosphorylation. Around m/z 3320 in Figure 2b, two main ion signals are observed. Their corresponding masses are 43075.35 and 43155.35 Da, a mass difference of 80.07 and 160.07 Da compared to the N-acetylated polypeptide backbone mass, respectively. These data indicate that the major ovalbumin species is diphosphorylated (77.3%), also with a quite abundant monophosphorylated proteoform (21.6%). In addition, we found a low abundant species (1.1%) corresponding to the nonphosphorylated ovalbumin. It is well-known from literature that ovalbumin bears only two residues that are highly phosphorylated (i.e., S68 and S344). Our results are quantitatively reasonably consistent with earlier studies by SDS−PAGE, reporting primarily diphosphorylation with monophosphorylation to be present for ∼34%.[18,19]

Analysis of Dephosphorylated Ovalbumin. After treatment by CIP, the baseline resolved spectrum of dephosphorylated ovalbumin displayed in Figure 2c presents ideal data to dissect the variation in glycosylation, which is the main cause of ovalbumin microheterogeneity. A comparison of the spectra of

dx.doi.org/10.1021/ac403057y | Anal. Chem. 2013, 85, 12037−12045

dephosphorylated (Figure 2c) and unprocessed ovalbumin (Figure 2a) reveals a clear reduction in the numbers of proteoforms caused by complete dephosphorylation. We calculated the mass of individual glycan structures by subtracting 42995.35 Da (the mass of the deglycosylated and dephosphorylated polypeptide backbone of ovalbumin) from each identified glycoform, and the mass of one GlcNAc (203.19) and the reduced N-terminus (18.01). Next, we constructed a mass difference matrix to identify relationships between any two detected masses, whereby an "exact" difference of one monosaccharide (hexose/Hex, *N*-acetylhexosamine/HexNAc, deoxyhexose/dHex, sialic acid/Sia) was considered a match. As is evident from Table 1, in total, an unprecedented number of 45 different compositions, built up from Hex and HexNAc units supplemented a few times with one or two Sia (= *N*-acetylneuraminic acid/Neu5Ac) residues, could be detected and assigned with satisfying accuracy. These glycan structures range in mass from about 1000 to 3500 Da and consist of 6 to 19 monosaccharide moieties. We also quantified all these glycoforms summing the ions signals over all observed charge states (Table 1). For less than half, i.e., 19 out of the 45 compositions (detected masses), glycan structures have been previously annotated in chicken ovalbumin (Table 1). Among the remaining 26, we found 7 compositions that fit reference structures as being reported for pigeon ovalbumin.[20]

Analysis of Unprocessed Ovalbumin. Evidently, it would be advantageous to analyze the microheterogeneity of endogenous proteins, avoiding the use of enzymes to cleave off some of the modifications, as in any of these processes information or sample can get lost. Moreover, the reproducibility of such procedures is not trivial. Obviously, the mass spectrum of unprocessed ovalbumin (Figures 1a and 2a) represents the most complex spectrum. In the spectra of unprocessed ovalbumin, we could readily separate by mass and distinguish around 60 different proteoforms. In Figure 3, we plotted as mirror images the zero-charge convoluted spectra of natural unprocessed ovalbumin (in blue) and dephosphorylated ovalbumin (in black). For a more clear comparison, the spectrum of unprocessed ovalbumin was shifted by 160 Da to lower mass, so that the doubly phosphorylated peaks in unprocessed ovalbumin align with their nonphosphorylated peaks in dephosphorylated ovalbumin. In Figure 3, the smaller peaks (above ~45000 Da) have been magnified by a factor of 10. Still they represent based on their mass shifts (see Table 1) genuine structures that correspond to glycan structures but also due to the fact that also these signals are responsive to the dephosphorylation by CIP in an alike manner as the more abundant signals. In these images all peaks that show reduced abundance or even disappear correspond to phosphorylated proteoforms. A minor caveat is that we cannot easily resolve the difference between two phosphorylations (160 Da) and one hexose residue (162 Da), resulting in partial overlap of different proteoforms. For example, in Figure 3, annotated glycoform 8 can also be assigned to glycoform 10, bearing a single phosphorylation on phosphorylation sites S68 or S344. After removal of the phosphate groups, the relative abundance of peak 10 reduces, indicating that this peak is most likely a mixture of two proteoforms: one is diphosphorylated ovalbumin with glycan 8 on glycosylation site N292, and the other is a singly phosphorylated ovalbumin bearing glycan 10. Such partial overlap could possibly induce the relatively large mass deviations observed for some glycan structures in Table 1 (composition numbers 3, 12, 15, 16, 19, 21, 24, 27, 40, and 44).

In summary, we profiled 59 different proteoforms in natural unprocessed chicken ovalbumin, including 45 proteoforms with different glycans, 13 monophosphorylated proteoforms, a few nonphosphorylated proteoforms, and a few wherein the N-acetylation was missing. The identified glycan masses ranged from about 1000 to 3500 Da, and their relative intensities spanned about 2 orders.

DISCUSSION

Qualitative and Semiquantitative Analysis of Proteoforms of Ovalbumin. The high-resolving power of the modified Exactive Orbitrap mass analyzer at elevated m/z allows confident separation and mass assignment of all the coappearing proteoforms in chicken ovalbumin, enabling qualitative structural analysis from a single spectrum in a matter of minutes, consuming only a few femtomoles of unprocessed analyte. Semiquantitative analysis of ovalbumin PTMs, such as N-acetylation cleavages, phosphorylation, and extensive glycosylation, are in satisfying agreement with previous studies using classical analytical techniques such as SDS−PAGE, CE, and MALDI-MS. Therefore, we consider our method based on high-resolution mass spectrometry as a confident strategy for the characterization of protein microheterogeneity. More than half of the identified proteoforms are present below a 5% relative abundance. Direct analysis toward these less-populated proteoforms would be much more difficult using traditional techniques based on bottom-up proteome analysis and chromatography, since information might be lost during the sample preparation, separation, or detection process.

Benchmarking against Reported Literature. Over the past decades, the N-glycosylation of chicken ovalbumin has been examined by a plethora of analytical techniques, making it already, before this study, one of the best-characterized glycoproteins.[21−57] In fact, the glycoprotein has been quite often selected as a model compound in the development of new strategies for the structural analysis of N-glycosylation patterns, making use of chemically or enzymatically released carbohydrate chains from denatured material. It should be noted that in most studies commercially available ovalbumin preparations have been used instead of highly purified samples. In view of this, it has been reported that among the many assigned glycan structures in the literature, several structures do not originate from ovalbumin but from contaminating glycoproteins, such as ovomucoid,[39,47,58−63] ovotransferrin,[32,39] or riboflavin-binding protein.[47,64,65] Although for our research we have used commercial chicken ovalbumin (grade V), our data exclude such possibilities; as by analyzing the intact glycoprotein instead of the released glycans, we unambiguously link the observed glycan compositional data to the ovalbumin polypeptide backbone. It should be noted that in our analysis we did not observe any traces of ovomucoid (28 kDa) or ovotransferrin (77 kDa), glycoproteins which should easily be mass-resolved from ovalbumin. For the majority of the 45 compositions in terms of $Sia_xHex_yHexNAc_z$, as presented in Table 1, we have shown the translation into real glycan structures based on Neu5Ac, Gal, Man, and GlcNAc, as available from the literature, in Figure S-2 of the Supporting Information. The symbolic notation of the N-glycan structures and linkages are explained in Supporting Information, Figure S-3. Most of the assigned structures are based on highly detailed previous studies on chicken ovalbumin using methylation analysis in combination with liquid chromatography/exoglycosidase digestions (composition numbers 1, 2, 4, 8, 10, 11, 14,

18, and 23),[24−27,36] NMR spectroscopy (composition numbers 1, 2, 4, 6−8, 10−12, 14−16, and 18),[29,31,32,34,35,39,42] two-dimensional (2D) high-performance liquid chromatography (HPLC) in combination with exoglycosidase digestions (composition numbers 2, 4, 6, 7, 8, 10, 11, 14, and 18),[37] MALDI-TOF MS in combination with exoglycosidase digestions, including NMR and enzymatic data of earlier reports (composition numbers 1−12, 14−16, 18, 19, and 22),[47] and detailed MS fragmentations studies (composition numbers 5, 6, and 10).[52] The references included in Table 1 and Figure S-2 of the Supporting Information refer to these original studies.

In a detailed study, Harvey et al.[47] compared the structures of the released glycans of commercial chicken ovalbumin (grade V) with those of HPLC-purified chicken ovalbumin and gave a list of glycans, which in their opinion were originating from contaminating glycoproteins. This holds especially for tetra-antennae (2,4 and 2,6 branching) and penta-antennae (2,4 and 2,4,6 branching) with intersecting GlcNAc being found in ovomucoid[58−63] and for some of the smaller structures. Their conclusion that the glycans related to the composition numbers 1, 3, 16, 19, and 22 do not belong to chicken ovalbumin is not in agreement with our findings. However there is NMR proof for a penta-antennary structure with intersecting GlcNAc for composition number 16 in chicken ovalbumin (grade V;[42] it could be that this structure, like all the other penta-antennary structures,[47] belongs to ovomucoid).[58,59] With some exceptions, as mentioned above, over the whole range our findings are consistent with the findings of Harvey et al. in terms of glycan structures, mass distribution, and even relative abundance. The five most abundant glycan structures they observed (numbered 4, 8, 15, 19/20, and 25 in their Figure 3a) also match the top 5 in our data (numbered 2, 4, 10, 14, and 18 in Table 1). It should be mentioned that they stated that the N-glycan profiles of the intact HPLC-purified chicken ovalbumin, as studied by ESI-MS, and the released glycans matched each other. Two earlier ESI-MS investigations on intact chicken ovalbumin showed only a small part of the 45 compositions found in our study. In the first study,[41] the composition numbers 2, 4, 10, 13, 14, and 18 (Table 1) were identified, and in the second study,[49] the composition numbers were 2, 4, 6, 8, 10, 12, 13, 14, 16, and 18 (Table 1) (the reported compositions $Hex_3HexNAc_4$ and $Hex_4HexNAc_7$ were not detected in our study).

Inspection of the presented glycans with composition numbers 1−23 (Table 1) confirmed the presence of oligomannose-type, hybrid-type with and without intersecting GlcNAc, and complex-type di-, tri- (2,4 or 2,6 branching), and tetra-antennary (2,4 and 2,6 branching) structures with intersecting GlcNAc. Inspection of the remaining composition numbers 24−45, primarily heavier in mass and more complex, accounting cumulatively for 4.1% of the total ion intensity in the unprocessed ovalbumin mass spectra, showed for the numbers 25, 27, 28, 30, 34, 37, and 44 a fit with glycan structures, earlier reported for pigeon ovalbumin (Table 1).[20] In the latter study, the assigned structures have been estimated by FAB-MS and ESI-MS in combination with methylation analysis and three-dimensional HPLC/exoglycosidase digestions and are part of a series of N-glycans containing terminal Gal(α1−4)Gal epitopes. These findings contradict previous suggestions claiming the total absence of Gal(α1−4)Gal entities in Galliformes (chicken).[66] We tried to confirm the Gal(α1−4)Gal structure using α(1−3,-4,-6)-galactosidase from coffee bean, but this enzyme did not show any activity to intact chicken ovalbumin under native conditions. Still, our data reveal that it is highly likely that several Gal(α1−4)Gal glycan structures in very minor amounts are present in chicken ovalbumin. We believe they have not been reported before by other techniques due to their very low relative abundance.

Another aspect, when trying to convert compositions in the range 24−45 to glycan structures, is the high number of HexNAc units. With a focus on composition number 36, $Hex_7HexNAc_9$ (i.e., $Gal_4Man_3GlcNAc_9$), it is clear that even suggesting penta-antennary (2,4 and 2,4,6 branching) structures with intersecting GlcNAc, a repeating Gal(β1−4)GlcNAc unit (polylactosamine type), should be present. Taking into account that penta-antennary structures (with and without intersecting GlcNAc) have been indicated not to belong to chicken ovalbumin, but for instance to contaminating chicken ovomucoid,[47] we hypothesize that several of the complex-type glycans in the composition range 24−45 are in fact extensions of the well-established complex-type glycans from the composition range 1−23, namely, with terminal Gal(α1−4)Gal and polylactosamine units, in separated or mixed form (see, for example, hypothetical tri- and tetra-antennary glycan structures with intersecting GlcNAc for composition number 36 in Figure S-4 of the Supporting Information).

Strengths and Limitations of the Approach. Compared to current analytical approaches for analyzing protein microheterogeneity, for instance by chromatographic-based techniques (SCX, HILIC), gel electrophoresis (SDS−PAGE, 2D gel), and capillary electrophoresis, high-resolution native ESI-MS separates proteoforms based on their mass. Our approach has some clear distinct advantages. First, it consumes very little sample and time to obtain reliable information. Second, it gives a panoramic view of all coappearing species, including low abundant ones. Third, it excludes possible interference from copurified contaminant proteins.

In contrast to classical glycan structure studies, we electrospray the intact protein instead of the released glycans or glycopeptides, measuring the mass shift between different glycoforms on the intact polypeptide backbone. In this way, we significantly reduce any bias induced by difference in the ionization efficiency toward different sugar residues (for example, sialic acid). Furthermore, incomplete digestion due to enzyme specificity is not a problem for the glycan assignment. In this way, it is possible to preserve comprehensive information even for lower abundant glycoforms. In principle, the analysis presented here could also be done by ESI-MS on denatured proteins, introduced into the mass spectrometer either by LC−MS or direct infusion. Certainly, the resolution of the Orbitrap and other FT mass analyzers is even higher in the lower m/z ranges, which is necessary to detect and resolve the highly charged proteins. As discussed above, ovalbumin sprayed from such a denaturing solution, typically used in MS, leads to a very broad charge envelope ranging from $[M + 18H]^{18+}$ to $[M + 45H]^{45+}$ (see Figure S-1 of the Supporting Information). The inherent disadvantages of using denaturing conditions include the following: (a) it is less "native" due to the loss of protein tertiary structure, (b) ion signals are spread out over more species, which reduces S/N, and (c) all ion signals appear in narrower m/z windows, making undesirable overlap more likely.

An obvious disadvantage of our strategy is that it is rather blind in assessing monosaccharide stereoisomers, type of

linkages, anomeric configurations, and glycan branching, which still would require dedicated glycan analysis by NMR spectroscopy, LC combined with exoglycosidases, and methylation analysis or MS/MS.

Future Perspective. Protein microheterogeneity resulting from genetic variants, RNA editing, cellular processing, or PTMs can affect protein activity and stability, also in the case of recombinant therapeutic proteins.[67−69] Therefore, analysis of protein microheterogeneity is crucial. Yet, it remains analytically challenging since it requires high-resolution separation techniques. We foresee that native ESI-MS using the modified Orbitrap Exactive high-resolution mass analyzer will make a significant contribution to the field, as demonstrated here by taking the prototypical endogenous protein ovalbumin as a model case. One single native ESI-MS spectrum reveals the masses and relative abundances of each co-occurring proteoform, providing a qualitative and semiquantitative fingerprint spectrum. This will allow analysis of any PTM (phosphorylation, glycosylation, lysine-acetylation, etc.) at the intact protein level. These analyses are applicable to any class of proteins and can complement typical top-down proteomics experiments. Especially, kinases, oncogenes, and chromatin-related proteins are known to be decorated by a plethora of functionally important PTMs, leading to rather complex protein microheterogeneity. The achieved high mass-resolving power and high mass accuracy allows for comprehensive, in-depth, and detailed parallel characterization of various modifications, contributing to our understanding of protein functioning in general.

CONCLUSIONS

Here, we present a new strategy to analyze protein microheterogeneity. Using a modified Orbitrap Exactive mass analyzer, we performed native MS experiments on intact chicken ovalbumin. An unprecedented number of around 60 proteoforms could be distinguished and baseline separated by mass. After enzymatic removal of part of the glycan chains and/or phosphate groups from intact ovalbumin, the microheterogeneity reduced extensively. All identified proteoforms, could not only be detected but also assigned and semiquantified. When structural data were available, our assignments were in good agreement with the literature. Furthermore, we also identified and assigned more than 20 previously unreported new glycan structures, providing evidence suggesting the existence of Gal(α1−4)Gal and polylactosamine type units, revealing novel aspects in the glycobiology of chicken ovalbumin.

ASSOCIATED CONTENT

Supporting Information

Additional information as noted in text. This material is available free of charge via the Internet at http://pubs.acs.org.

AUTHOR INFORMATION

Corresponding Author

*E-mail: a.j.r.heck@uu.nl.

Notes

The authors declare no competing financial interest.

ACKNOWLEDGMENTS

This work, and in particular Y.Y. and A.J.R.H., has been supported by the ManiFold project, Grant 317371, and in part by the PRIME-XS project, Grant 262067, both funded by the European Union seventh Framework Programme. The Netherlands Proteomics Center, embedded in The Netherlands Genomics Initiative, is acknowledged for funding.

REFERENCES

(1) Nisbet, A. D.; Saundry, R. H.; Moir, A. J. G.; Fothergill, L. A.; Fothergill, J. E. *Eur. J. Biochem.* **1981**, *115* (2), 335−345.
(2) Huntington, J. A.; Stein, P. E. *J. Chromatogr., B* **2001**, *756* (1−2), 189−198.
(3) Bushey, M. M.; Jorgenson, J. W. *Anal. Chem.* **1990**, *62* (10), 978−984.
(4) Wagner, K.; Racaityte, K.; Unger, K. K.; Miliotis, T.; Edholm, L. E.; Bischoff, R.; Marko-Varga, G. *J. Chromatogr., A* **2000**, *893* (2), 293−305.
(5) Landers, J. P.; Oda, R. P.; Madden, B. J.; Spelsberg, T. C. *Anal. Biochem.* **1992**, *205* (1), 115−124.
(6) Dickerson, J. A.; Ramsay, L. M.; Dada, O. O.; Cermak, N.; Dovichi, N. J. *Electrophoresis* **2010**, *31* (15), 2650−2654.
(7) Di Palma, S.; Hennrich, M. L.; Heck, A. J. R.; Mohammed, S. *J. Proteomics* **2012**, *75* (13), 3791−3813.
(8) Danzo, B. J.; Bell, B. W. *J. Biol. Chem.* **1988**, *263* (5), 2402−2408.
(9) Rose, R. J.; Damoc, E.; Denisov, E.; Makarov, A.; Heck, A. J. R. *Nat. Methods* **2012**, *9* (11), 1084−1086.
(10) Ceroni, A.; Maass, K.; Geyer, H.; Geyer, R.; Dell, A.; Haslam, S. M. *J. Proteome Res.* **2008**, *7* (4), 1650−1659.
(11) Stein, P. E.; Leslie, A. G. W.; Finch, J. T.; Carrell, R. W. *J. Mol. Biol.* **1991**, *221* (3), 941−959.
(12) Tarentino, A. L.; Gomez, C. M.; Plummer, T. H. *Biochemistry* **1985**, *24* (17), 4665−4671.
(13) Trimble, R. B.; Tarentino, A. L. *J. Biol. Chem.* **1991**, *266* (3), 1646−1651.
(14) Tarentino, A. L.; Plummer, T. H., Jr. *Methods Enzymol.* **1994**, *230*, 44−57.
(15) Plummer, T. H., Jr.; Tarentino, A. L. *Glycobiology* **1991**, *1* (3), 257−263.
(16) Woo, S. L. C.; Beattie, W. G.; Catterall, J. F.; Dugaiczyk, A.; Staden, R.; Brownlee, G. G.; O'Malley, B. W. *Biochemistry* **1981**, *20* (22), 6437−46.
(17) Palmiter, R. D.; Gagnon, J.; Walsh, K. A. *Proc. Natl. Acad. Sci. U.S.A.* **1978**, *75* (1), 94−98.
(18) Kinoshita-Kikuta, E.; Kinoshita, E.; Koike, T. *Electrophoresis* **2012**, *33* (5), 849−855.
(19) Wei, J.; Yang, L.; Harrata, A. K.; Lee, C. S. *Electrophoresis* **1998**, *19* (13), 2356−2360.
(20) Takahashi, N.; Khoo, K.-H.; Suzuki, N.; Johnson, J. R.; Lee, Y. C. *J. Biol. Chem.* **2001**, *276* (26), 23230−23239.
(21) Cunningham, L.; Ford, J. D.; Rainey, J. M. *Biochim. Biophys. Acta* **1965**, *101* (2), 233−235.
(22) Huang, C.-C.; Mayer, H. E., Jr; Montgomery, R. *Carbohydr. Res.* **1970**, *13* (1), 127−137.
(23) Tarentino, A. L.; Plummer, T. H., Jr.; Maley, F. *J. Biol. Chem.* **1972**, *247* (8), 2629−2631.
(24) Tai, T.; Yamashita, K.; Ogata-Arakawa, M.; Koide, N.; Muramatsu, T.; Iwashita, S.; Inoue, Y.; Kobata, A. *J. Biol. Chem.* **1975**, *250* (21), 8569−8575.
(25) Tai, T.; Yamashita, K.; Ito, S.; Kobata, A. *J. Biol. Chem.* **1977**, *252* (19), 6687−6694.
(26) Tai, T.; Yamashita, K.; Kobata, A. *Biochem. Biophys. Res. Commun.* **1977**, *78* (1), 434−441.
(27) Yamashita, K.; Tachibana, Y.; Kobata, A. *J. Biol. Chem.* **1978**, *253* (11), 3862−3869.
(28) Conchie, J.; Strachan, I. *Carbohydr. Res.* **1978**, *63*, 193−213.
(29) Narasimhan, S.; Harpaz, N.; Longmore, G.; Carver, J. P.; Grey, A. A.; Schachter, H. *J. Biol. Chem.* **1980**, *255* (10), 4876−4884.
(30) Atkinson, P. H.; Grey, A.; Carver, J. P.; Hakimi, J.; Ceccarini, C. *Biochemistry* **1981**, *20* (14), 3979−3986.

(31) Carver, J. P.; Grey, A. A.; Winnik, F. M.; Hakimi, J.; Ceccarini, C.; Atkinson, P. H. *Biochemistry* **1981**, *20* (23), 6600−6606.
(32) Longmore, G. D.; Schachter, H. *Carbohydr. Res.* **1982**, *100*, 365−392.
(33) Yamashita, K.; Ueda, I.; Kobata, A. *J. Biol. Chem.* **1983**, *258* (23), 14144−14147.
(34) Ceccarini, C.; Lorenzoni, P.; Atkinson, P. H. *Biochim. Biophys. Acta* **1983**, *759* (3), 214−221.
(35) Nomoto, H.; Inoue, Y. *Eur. J. Biochem.* **1983**, *135* (2), 243−250.
(36) Yamashita, K.; Tachibana, Y.; Hitoi, A.; Kobata, A. *Carbohydr. Res.* **1984**, *130*, 271−288.
(37) Tomiya, N.; Awaya, J.; Kurono, M.; Endo, S.; Arata, Y.; Takahashi, N. *Anal. Biochem.* **1988**, *171* (1), 73−90.
(38) Chen, L. M.; Yet, M. G.; Shao, M. C. *FASEB J.* **1988**, *2* (12), 2819−2824.
(39) Nomoto, H.; Yasukawa, K.; Inoue, Y. *Biosci. Biotechnol. Biochem.* **1992**, *56* (7), 1090−1095.
(40) Rago, R. P.; Ramirez-Soto, D.; Poretz, R. D. *Carbohydr. Res.* **1992**, *236*, 1−8.
(41) Duffin, K. L.; Welply, J. K.; Huang, E.; Henion, J. D. *Anal. Chem.* **1992**, *64* (13), 1440−1448.
(42) Corradi Da Silva, M. L.; Stubbs, H. J.; Tamura, T.; Rice, K. G. *Arch. Biochem. Biophys.* **1995**, *318* (2), 465−475.
(43) North, S.; Okafo, G.; Birrell, H.; Haskins, N.; Camilleri, P. *Rapid Commun. Mass Spectrom.* **1997**, *11* (15), 1635−1642.
(44) North, S.; Birrell, H.; Camilleri, P. *Rapid Commun. Mass Spectrom.* **1998**, *12* (7), 349−356.
(45) Anumula, K. R.; Dhume, S. T. *Glycobiology* **1998**, *8* (7), 685−694.
(46) Mechref, Y.; Novotny, M. V. *Anal. Chem.* **1998**, *70* (3), 455−463.
(47) Harvey, D. J.; Wing, D. R.; Küster, B.; Wilson, I. B. H. *J. Am. Soc. Mass Spectrom.* **2000**, *11* (6), 564−571.
(48) Charlwood, J.; Birrell, H.; Bouvier, E. S. P.; Langridge, J.; Camilleri, P. *Anal. Chem.* **2000**, *72* (7), 1469−1474.
(49) Saba, J. A.; Shen, X.; Jamieson, J. C.; Perreault, H. *J. Mass Spectrom.* **2001**, *36* (5), 563−574.
(50) An, H. J.; Peavy, T. R.; Hedrick, J. L.; Lebrilla, C. B. *Anal. Chem.* **2003**, *75* (20), 5628−5637.
(51) Lattova, E.; Perreault, H. *J. Chromatogr., A* **2003**, *1016* (1), 71−87.
(52) Lattova, E.; Perreault, H.; Krokhin, O. *J. Am. Soc. Mass Spectrom.* **2004**, *15* (5), 725−735.
(53) Lattová, E.; Snovida, S.; Perreault, H.; Krokhin, O. *J. Am. Soc. Mass Spectrom.* **2005**, *16* (5), 683−696.
(54) Plasencia, M. D.; Isailovic, D.; Merenbloom, S. I.; Mechref, Y.; Clemmer, D. E. *J. Am. Soc. Mass Spectrom.* **2008**, *19* (11), 1706−1715.
(55) Gil, G.-C.; Kim, Y.-G.; Kim, B.-G. *Anal. Biochem.* **2008**, *379* (1), 45−59.
(56) Qin, H.; Zhao, L.; Li, R.; Wu, R.; Zou, H. *Anal. Chem.* **2011**, *83* (20), 7721−7728.
(57) Jeong, H.-J.; Kim, Y.-G.; Yang, Y.-H.; Kim, B.-G. *Anal. Chem.* **2012**, *84* (7), 3453−3460.
(58) Yamashita, K.; Kamerling, J. P.; Kobata, A. *J. Biol. Chem.* **1982**, *257* (21), 12809−12814.
(59) Paz-Parente, J.; Wieruszeski, J. M.; Strecker, G.; Montreuil, J.; Fournet, B.; van Halbeek, H.; Dorland, L.; Vliegenthart, J. F. G. *J. Biol. Chem.* **1982**, *257* (22), 13173−13176.
(60) Yamashita, K.; Kamerling, J. P.; Kobata, A. *J. Biol. Chem.* **1983**, *258* (5), 3099−3106.
(61) Paz-Parente, J.; Strecker, G.; Leroy, Y.; Montreuil, J.; Fournet, B.; van Halbeek, H.; Dorland, L.; Vliegenthart, J. F. G. *FEBS Lett.* **1983**, *152* (2), 145−152.
(62) Egge, H.; Peter-Katalinić, J.; Paz-Parente, J.; Strecker, G.; Montreuil, J.; Fournet, B. *FEBS Lett.* **1983**, *156* (2), 357−362.
(63) Dorland, L.; Haverkamp, J.; Vliegenthart, J. F. G.; Spik, G.; Fournet, B.; Montreuil, J. *Eur. J. Biochem.* **1979**, *100* (2), 569−574.
(64) Piskarev, V. E.; Sepetov, N. F.; Likhosherstov, L. M.; Galenko, E. L.; Derevitskaia, V. A.; Kochetkov, N. K. *Russ. J. Bioorg. Chem.* **1989**, *15* (11), 1546−1554.
(65) Likhosherstov, L. M.; Piskarev, V. E.; Sepetov, N. F.; Derevitskaia, V. A.; Kochetkov, N. K. *Russ. J. Bioorg. Chem.* **1991**, *17* (2), 246−251.
(66) Suzuki, N.; Laskowski, M., Jr; Lee, Y. C. *Proc. Natl. Acad. Sci. U.S.A.* **2004**, *101* (24), 9023−9028.
(67) Schweigert, F. J. *Briefings Funct. Genomics Proteomics* **2005**, *4* (1), 7−15.
(68) Fekete, S.; Gassner, A.-L.; Rudaz, S.; Schappler, J.; Guillarme, D. *Trends. Anal. Chem.* **2013**, *42*, 74−83.
(69) Chen, G.; Warrack, B. M.; Goodenough, A. K.; Wei, H.; Wang-Iverson, D. B.; Tymiak, A. A. *Drug Discovery Today* **2011**, *16* (1−2), 58−64.